Evidence of a triosephosphate isomerase non-catalytic function crucial to behavior and longevity

Bartholomew P. Roland[1,2,3], Kimberly A. Stuchul[1,2], Samantha B. Larsen[1,2], Christopher G. Amrich[4], Andrew P. VanDemark[4], Alicia M. Celotto[1,2] and Michael J. Palladino[1,2,*]

[1]Department of Pharmacology and Chemical Biology, University of Pittsburgh School of Medicine, Pittsburgh, PA 15261, USA
[2]Pittsburgh Institute for Neurodegenerative Diseases, University of Pittsburgh School of Medicine, Pittsburgh, PA 15261, USA
[3]Molecular Pharmacology Graduate Training Program, University of Pittsburgh School of Medicine, Pittsburgh, PA 15261, USA
[4]Department of Biological Sciences, University of Pittsburgh, Pittsburgh, PA 15260, USA

*Author for correspondence (mjp44@pitt.edu)

Accepted 4 April 2013
Journal of Cell Science 126, 3151–3158

doi: 10.1242/jcs.124586

Summary

Triosephosphate isomerase (TPI) is a glycolytic enzyme that converts dihydroxyacetone phosphate (DHAP) into glyceraldehyde 3-phosphate (GAP). Glycolytic enzyme dysfunction leads to metabolic diseases collectively known as glycolytic enzymopathies. Of these enzymopathies, TPI deficiency is unique in the severity of neurological symptoms. The *Drosophila sugarkill* mutant closely models TPI deficiency and encodes a protein prematurely degraded by the proteasome. This led us to question whether enzyme catalytic activity was crucial to the pathogenesis of *TPI sugarkill* neurological phenotypes. To study TPI deficiency *in vivo* we developed a genomic engineering system for the *TPI* locus that enables the efficient generation of novel *TPI* genetic variants. Using this system we demonstrate that *TPI sugarkill* can be genetically complemented by *TPI* encoding a catalytically inactive enzyme. Furthermore, our results demonstrate a non-metabolic function for TPI, the loss of which contributes significantly to the neurological dysfunction in this animal model.

Key words: TPI, Triosephosphate isomerase, *Drosophila melanogaster*, Glycolysis, Longevity, Locomotor function

Introduction

Triosephosphate isomerase (TPI) is a homodimeric enzyme that functions in a non-linear step of glycolysis, converting dihydroxyacetone phosphate (DHAP) into glyceraldehyde 3-phosphate (GAP). Both DHAP and GAP are produced from the catabolism of fructose 1,6-bisphosphate by the enzyme aldolase; however, only GAP can be utilized by the remaining steps in glycolysis. Therefore, TPI is responsible for the net gain of glycolysis-derived ATP as well as the production of an extra molecule of pyruvate per molecule of glucose. This enhancement of glycolysis is important in the bioenergetics of both aerobic and anaerobic metabolism.

TPI deficiency is a recessive loss-of-function human disease resulting from missense mutations in the *TPI* gene. TPI deficiency is clinically characterized by symptoms such as hemolytic anemia, cardiomyopathy, neurological dysfunction and degeneration, and premature death (Schneider, 2000; Orosz et al., 2006). Pathogenic TPI deficiency mutations can affect the promoter or coding sequence and all have been reported to dramatically reduced TPI activity owing to changes in catalysis and/or enzyme stability (Daar et al., 1986; Hollán et al., 1993; Arya et al., 1997). TPI deficiency has a very poor genotype-phenotype correlation and studies to elucidate pathogenesis are extremely limited, especially in animal systems.

Drosophila are the only model system identified to date in which mutants have been shown to recapitulate the neurological phenotypes seen in human patients (Celotto et al., 2006; Gnerer et al., 2006). We have previously isolated an animal model of TPI deficiency known as $TPI^{sugarkill\ (sgk)}$. TPI^{sgk} is characterized by shortened lifespan, neurodegeneration, and conditional behavioral abnormalities (Celotto et al., 2006) resulting from a missense mutation causing a methionine to threonine substitution (M80T). The affected methionine is present near the dimer interface yet does not seem to result in a shift in monomer-dimer populations *in vivo* (Seigle et al., 2008). However, the TPI^{sgk} mutation has been shown to induce abnormal proteasomal degradation of TPI resulting in reduced total TPI protein (Seigle et al., 2008; Hrizo and Palladino, 2010). Interestingly, we have previously shown that this loss-of-function mutation can be attenuated by overexpressing mutant TPI^{sgk} (Celotto et al., 2006). This result led us to question whether the presence of the enzyme or its catalytic activity was most important to the pathogenesis of *sugarkill*. Here we demonstrate that the M80T substitution in TPI^{sgk} reduces its isomerase activity and, based on the proximity to one of the TPI catalytic sites, we predict that the reduced catalytic efficiency is a result of the influence of the mutation on dimeric cooperation.

To address whether the presence of the enzyme or its catalysis were most important to the TPI^{sgk} disease phenotypes *in vivo*, we developed genomic engineering (GE) of the *Drosophila TPI* locus. This process establishes an *attP ΔTPI* founder line which can be used to modify the gene locus using highly efficient *attP/attB* transgenesis. We hypothesized that if the presence of the enzyme was crucial to pathogenesis independent of catalytic activity, we would be able to rescue the disease phenotypes with a catalytically inactive variant of the protein. Lys11 of TPI is a

fully conserved catalytic residue known to be required for substrate binding and substitution to Met completely abolishes catalysis (Lodi et al., 1994; Wierenga et al., 2010). We have generated the *attP ΔTPI* founder line and have used GE to create *Drosophila* TPI^{K11M}, encoding a catalytically inactive TPI. Here we demonstrate that TPI^{K11M} genetically complements the longevity and behavior of the TPI^{sgk} animal model of TPI deficiency. Furthermore, catalytically inactive TPI complements TPI^{sgk} phenotypes without enhancing its stability, catalysis or reducing the associated metabolic stress. Collectively, these data suggest a function of TPI independent of its catalytic activity which is crucial to behavior and longevity.

Results

Recombinant TPI enzyme activity

Previous studies established that TPI^{sgk} is a recessive loss-of-function mutation characterized by reduced TPI levels (Seigle et al., 2008). Genetic data suggested that TPI^{sgk} retained sufficient function to rescue mutant survival and behavioral phenotypes if overexpressed (Seigle et al., 2008). These data led us to hypothesize that reduced TPI catalysis was crucial to the pathogenesis of TPI deficiency. To investigate this hypothesis further we generated recombinant *Drosophila* WT (dWT) and TPI^{sgk} (dM80T) and examined the kinetics of isomerase activity for each enzyme (Table 1). These data demonstrate that TPI^{sgk} (dM80T) exhibits a substantial reduction in isomerase activity. The dM80T protein has a 33% decrease in substrate affinity and ~11-fold reduction in catalytic activity compared to WT enzyme. This ultimately resulted in a ~15-fold reduction in enzyme efficiency. Both enzymes displayed typical Michaelis–Menten kinetics (supplementary material Fig. S1).

To assess the role of the M80 position within TPI function, we analyzed the crystal structure of TPI from *G. gallus* (Zhang et al., 1994) – *Drosophila* TPI shows 67% identity and 80% functional conservation with *G. gallus*. This structure was determined in the presence of the transition-state analog phosphoglycolohydroxamic acid (PGH), and the homologous methionine (M81) is located within the third loop of TPI (residues 63 to 86; Fig. 1A). This loop coordinates numerous interactions within the dimerization interface of TPI including important contacts between M81 and M13 and N14 of the neighboring subunit (Fig. 1B). These hydrophobic interactions help position the third loop, and are aided by hydrogen bonding between residues T74 and Q76 (also on the third loop), which interact with H94 and R97, respectively. The sum of these interactions is a coordinated network using conserved residues to mediate both hydrophobic and hydrogen-bonding interactions that ultimately positions both K11 and H94 properly within the active site of the enzyme (Fig. 1B,C). These residues are crucial for enzymatic function in TPI (Lambeir et al., 1987; Norledge et al., 2001) and establish a connection between M80 in *Drosophila* TPI and reduced catalysis for TPI^{sgk}.

Table 1. Kinetic parameters of *Drosophila* wild-type (dWT) and *sugarkill* (dM80T) triosephosphate isomerase enzymes

	dWT	dM80T
k_{cat} (GAP) (s^{-1})	1454±163.6	129.6±1.5
K_m (GAP) (mM)	2.8±0.4	3.7±0.5
k_{cat}/K_m (GAP) ($s^{-1}M^{-1}$)	5.2×10^5	3.5×10^4

dWT, *Drosophila* wild-type triosephosphate isomerase; dM80T, *Drosophila sugarkill* triosephosphate isomerase.
Values for $k_{cat\ and}$ K_m are means ± s.e.m.

Establishing that TPI^{sgk} still retained isomerase activity supported a catalytic explanation of our phenotypic attenuation via TPI^{sgk} transgenic overexpression. However, a rigorous assessment of this hypothesis *in vivo* would require supplementation of TPI levels without changing isomerase activity.

Generation of the founder knockout line by homologous recombination

To create a catalytically inactive allele of *TPI* we developed a GE approach for the *TPI* locus. Homologous recombination (HR) in *Drosophila* had previously been developed (Rong and Golic, 2000; Gong and Golic, 2003) but recent advances in GE technology have made the process considerably more efficient (Huang et al., 2008; Huang et al., 2009). The GE founder line was generated through replacement of the endogenous *TPI* locus using ends-out homologous recombination with a functional *attP* element (supplementary material Fig. S2A). *TPI* is located on the third chromosome between *CG31029* (centromeric) and *AdoR* (telomeric). Homology arms directing the deletion of the entire *TPI* locus were PCR amplified from the w^{1118} wild type genomic DNA and cloned into the *pGX-attP* targeting vector. Traditional P-element transgenesis was used to obtain *pGX-attP* insertion on the second chromosome. HR was induced as previously outlined (Huang et al., 2009). Approximately four hundred putative positive HR events were identified after screening ~60,000 animals. Among the putative positives, three positive HR lines were identified and verified using genetic and molecular methods.

Genetic validation included failure to complement a previously identified TPI null allele, TPI^{JS10} (Celotto et al., 2006), and homozygous lethality. Molecular validation included PCR analyses to confirm proper targeting of left and right homology arms using primers directed outside the homology arms and within construct elements. The confirmed founder line was reduced to remove w^{mc+} using a CRE recombinase and is designated *attP ΔTPI* (supplementary material Fig. S2B). The entire *attP ΔTPI* region was sequenced to confirm the correct placement of the GE elements and the integrity of the homology arms.

GE was performed to create TPI^{+} (*attR*), TPI^{+}-*CFP* (*attR*), TPI^{M80T} (*attR*), TPI^{K11M} (*attR*), *and* TPI^{K11M}-*CFP* (*attR*) animals using standard phiC31 site-directed integration followed by CRE-mediated reduction to remove w^{mc+} (supplementary material Fig. S2). These animals were molecularly verified using PCR analyses of the *attR* construct element (supplementary material Fig. S2E) and the locus was sequenced. Importantly, GE TPI^{+} (*attR*) animals are homozygous viable and behave normally while animals bearing the M80T substitution are substantially stress sensitive and exhibit reduced longevity (supplementary material Fig. S3). Animals homozygous for TPI^{K11M} (*attR*) are lethal, indicating a necessity for TPI catalysis during development.

Animal behavior and longevity

To test whether TPI isomerase activity was crucial to disease pathogenesis, TPI^{sgk}/TPI^{+}, TPI^{sgk}/TPI^{sgk}, TPI^{sgk}/TPI^{JS10}, and TPI^{sgk}/TPI^{K11M} animals were collected and aged at 25°C. TPI^{JS10} is a null allele owing to a 1.6 kb deletion, therefore TPI^{sgk}/TPI^{JS10} animals represent approximately the amount of TPI produced by one allele of TPI^{sgk}. For the purposes of this study, contrasting TPI^{sgk}/TPI^{JS10} with TPI^{sgk}/TPI^{K11M} provides

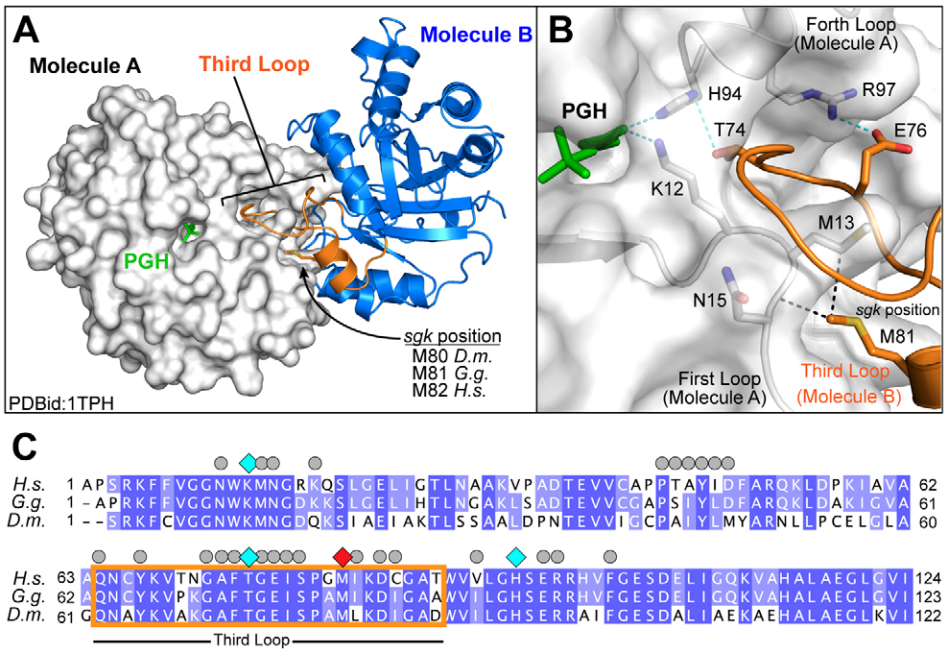

Fig. 1. Positioning of the third loop forms an interaction network connecting the dimerization interface to the catalytic pocket. (**A**) The crystal structure of TPI dimer from *Gallus gallus* (Protein Database ID: 1TPH). Monomer A of the dimer is rendered as a surface and colored white, whereas monomer B is shown as a cartoon colored blue, with the third loop highlighted in orange. The position of the transition state analog phosphoglycolohydroxamic acid (PGH, green) is indicated within the catalytic pocket. (**B**) Local environment of the third loop. Colored as before, with residues making important contributions to the dimerization interface indicated as sticks. Van der Waals interactions between M81 and residues M13 and N14 are indicated as black dotted lines. Hydrogen bonds between residues on the distal end of the third loop and connecting to the catalytic core are shown as green dotted lines. Residues are numbered based on the *Gallus gallus* sequence and for clarity we are using the TPI numbering standard lacking the initiator methionine. (**C**) An alignment of TPI protein sequences from *H. sapiens*, *G. gallus*, and *D. melanogaster*. Protein alignment was performed using the ClustalW method, with *H. sapiens* and *G. gallus* sharing 63.5% and 67.3% identity with *D. melanogaster*. Residues that mediate TPI dimerization are indicated by grey circles. Residues within the hydrogen-bonding network crucial for catalysis are indicated by cyan diamonds. The position of the *sugarkill* mutant (M81, red) and its positions within the third loop are indicated by an orange box.

the most informative comparison, as each animal population contains one catalytically active *TPI* allele.

Male and female animals were housed in vials of 10–20 individuals and examined for mechanical- and temperature-dependent locomotor defects on days 3 and 20. Time to recovery and time to paralysis were measured in each assay. While TPI^{sgk}/TPI^{+} shows no sign of paralysis or seizures upon mechanical stress, TPI^{sgk}/TPI^{sgk} and TPI^{sgk}/TPI^{JS10} exhibit a clear delay in recovery (Fig. 2A). In contrast, TPI^{sgk}/TPI^{K11M} animals display no signs of stress sensitivity (Fig. 2A). Previously, we have shown that TPI^{sgk} phenotypes are progressive in nature (Celotto et al., 2006; Seigle et al., 2008). We measured these behaviors at two time points, day 3 and day 20, to reveal whether TPI^{K11M} fully complements the TPI^{sgk} phenotypes or simply delays their onset. The catalytically inactive enzyme was shown to complement the mechanical stress sensitivity at both time points indicating that the TPI^{K11M} allele does not simply delay the progression of the disease phenotype (Fig. 2A).

Thermal stress sensitivity of the animals was also evaluated to test the possibility of pathogenic divergence (Fig. 2B). Here,

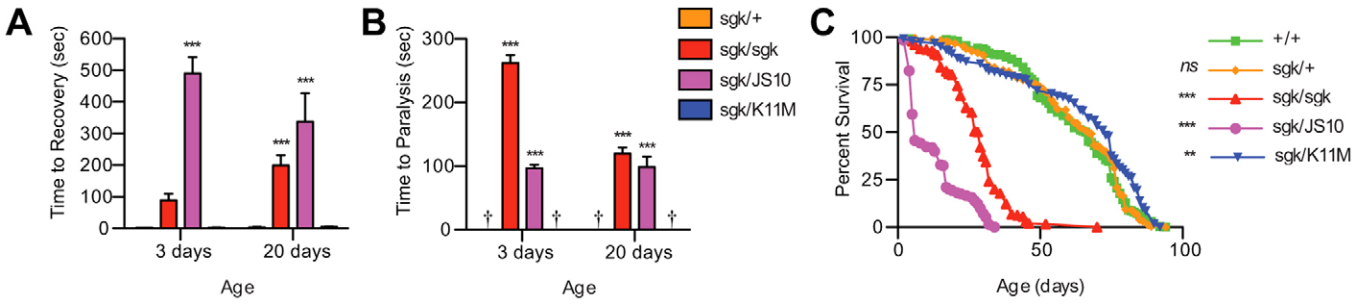

Fig. 2. The catalytically inactive TPI^{K11M} rescues behavioral and longevity phenotypes in TPI^{sgk}. (**A**) TPI^{K11M} complements TPI^{sgk} mechanical stress sensitivity at both day 3 and day 20. (**B**) TPI^{K11M} expression complements TPI^{sgk} thermal stress sensitivity, again at both day 3 and day 20. † indicates TPI^{sgk}/TPI^{+} and TPI^{sgk}/TPI^{K11M} animals were not paralyzed. (**C**) TPI^{K11M} complements the longevity defect of TPI^{sgk}. $^{**}P<0.01$ and $^{***}P<0.001$ relative to TPI^{+}/TPI^{+}; $n>15$ per genotype for all behavioral assays, and $n>150$ per genotype for all lifespans. Error bars indicate ± s.e.m.

TPI^{sgk}/TPI^{+} shows no signs of paralysis or seizures upon thermal stress, while TPI^{sgk}/TPI^{sgk} and TPI^{sgk}/TPI^{JS10} animals show distinct paralytic phenotypes initiated at ~240 seconds and ~90 seconds, respectively (Fig. 2B). In contrast, animals expressing the catalytically inactive allele TPI^{sgk}/TPI^{K11M} displayed no signs of paralysis after thermal stress induction (Fig. 2B). Again, we measured these behaviors at two time points, day 3 and day 20, and expression of the catalytically inactive enzyme was shown to complement the thermal stress sensitivity at both time points (Fig. 2B).

To test whether genetic complementation extended to longevity we performed lifespans as previously described (Palladino et al., 2003). TPI^{sgk} animals exhibit a marked reduction in median longevity that was also complemented with the catalytically inactive TPI^{K11M} allele (Fig. 2C; supplementary material Table S1). Finally, all genotypes eclosed at Mendelian rates suggesting the absence of developmental deficits and that the behavior of the adult population is representative of the genotype as a whole. These data show that expression of a catalytically inactive TPI is sufficient to rescue animal behavior and longevity in the TPI^{sgk} model of TPI deficiency.

TPI^{sgk} animal bioenergetics and lysate enzyme activity

Genetic complementation with TPI^{K11M} could indicate a previously unidentified non-isomerase function of the enzyme or it could result from a restoration of isomerase activity by a number of possible mechanisms. Thus, we examined whether TPI^{K11M} provided genetic complementation through a restoration of enzyme isomerase activity. TPI enzyme activity was robust in both TPI^{+}/TPI^{+} and TPI^{sgk}/TPI^{+} lysates yet markedly reduced in TPI^{sgk}/TPI^{sgk} and TPI^{sgk}/TPI^{JS10} animals (Fig. 3A). Most importantly, TPI^{sgk}/TPI^{K11M} animals exhibit levels of isomerase activity similar to TPI^{sgk}/TPI^{sgk} and TPI^{sgk}/TPI^{JS10} animals demonstrating that the genetic complementation is independent of isomerase activity (Fig. 3A).

The dramatic reduction in lysate isomerase activity suggested that pathogenesis of TPI^{sgk} neurological phenotypes could be unrelated to animal metabolic stress. Previous studies measuring ATP levels in this same mutant have failed to detect a significant change (Gnerer et al., 2006). To further evaluate the relationship between metabolism and TPI deficiency behavioral and longevity phenotypes we measured phosphorylated arginine [P-arg] to arginine [arg] concentration ratios as previously described (Viant et al., 2001), as this is an extremely sensitive assay of *Drosophila* bioenergetic status (Celotto et al., 2011). [P-arg]/[arg] ratios in TPI^{sgk} mutant animals were depressed compared to wild type, consistent with a strong loss-of-function mutation in glycolysis (Fig. 3B). This represents a reduction in the available pool of [P-arg] normalized to the total [arg] available, and suggests that the animals are utilizing this pool at a higher rate to buffer their ATP levels, similar to how mammals utilize phosphocreatine (Celotto et al., 2011). Importantly, TPI^{sgk}/TPI^{K11M} animals exhibiting low levels of catalytic activity also showed a similar depression in their [P-arg]/[arg] ratios compared to wild type animals (Fig. 3B). These data corroborate the lysate catalysis results and collectively indicate that TPI^{K11M} complements TPI^{sgk} phenotypes by a mechanism independent of the well-established role of TPI in cellular bioenergetics, and may provide an explanation as to the absence of an association between enzyme catalysis and neurological complications in human patients.

TPI^{sgk} and TPI^{K11M} protein levels

The capacity of a catalytically inactive allele of *TPI* to genetically complement all behavioral and longevity phenotypes independent of isomerase activity and animal metabolism strongly supports the conclusion that TPI^{sgk} phenotypes are due to a change in total TPI protein levels, not a reduction in TPI catalytic capacity. To determine whether the catalytically inactive TPI rescues total TPI levels, we immunoblotted for the presence of TPI with or without a cyan fluorescent protein (CFP) tag; the use of the tag allowed us to discriminate between protein isoforms. The addition of this C-terminal CFP does not influence the capacity of TPI^{K11M} to complement TPI^{sgk} phenotypes (supplementary material Fig. S4). TPI^{sgk} animals display reduced TPI protein levels *in vivo* (Seigle et al., 2008; Hrizo and Palladino, 2010), and TPI levels were further reduced when TPI^{sgk} was paired with the TPI^{JS10} null allele (Fig. 4A,C). Interestingly, complementing TPI^{sgk} with the catalytically inactive allele TPI^{K11M} rescues total TPI protein levels to that seen in the aphenotypic TPI^{+}/TPI^{+} wild type homozygotes. Observing $TPI^{K11M\text{-}CFP}$ and TPI^{sgk} independently, it can be seen that $TPI^{K11M\text{-}CFP}$ fails to change TPI^{sgk} levels relative to TPI^{sgk}/TPI^{JS10} or TPI^{sgk}/TPI^{sgk} (Fig. 4A,C) and, conversely, mutant TPI^{sgk} protein does not induce the degradation of $TPI^{K11M\text{-}CFP}$ relative to $TPI^{+}/TPI^{K11M\text{-}CFP}$ (Fig. 4B,C).

The inability of $TPI^{K11M\text{-}CFP}$ to modulate TPI^{sgk} levels suggests that any phenotypic rescue is likely being performed by the catalytically inactive isoform, and not merely increasing the presence of a still catalytically active TPI^{sgk}. Secondly, it is of particular interest that TPI^{sgk} does not significantly influence the levels of $TPI^{K11M\text{-}CFP}$. These results suggest three possible interpretations: (1) TPI^{sgk} is degraded prior to but stable upon heterodimerization; (2) TPI^{sgk} monomers are selectively degraded from heterodimer complexes; or (3) that TPI^{sgk} and

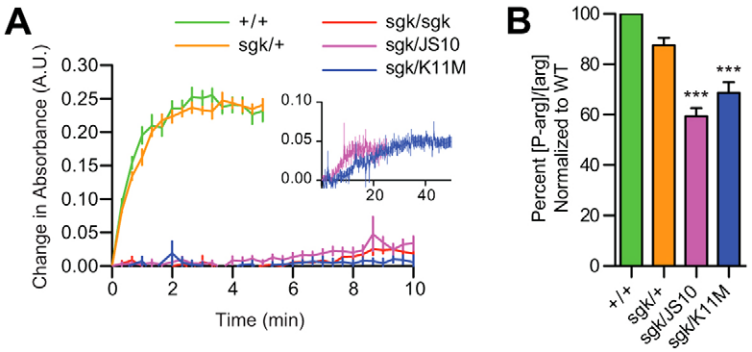

Fig. 3. TPI^{K11M} fails to rescue animal bioenergetics and TPI enzyme activity. (**A**) TPI^{sgk} exhibits little activity in animal lysates. Additionally, complementing TPI^{sgk} with TPI^{K11M} does not rescue its activity *in vivo*. Inset: a comparison between TPI^{sgk}/TPI^{JS10} and TPI^{sgk}/TPI^{K11M} lysate kinetics reveals low activity levels in both lysates (note that the units are the same but the scale has been changed). (**B**) TPI^{sgk}/TPI^{JS10} animals and TPI^{sgk}/TPI^{K11M} animals both showed reduced ratios of P-arg/arginine indicating bioenergetic stress. ***$P<0.001$ relative to WT. Error bars indicate ± s.e.m.

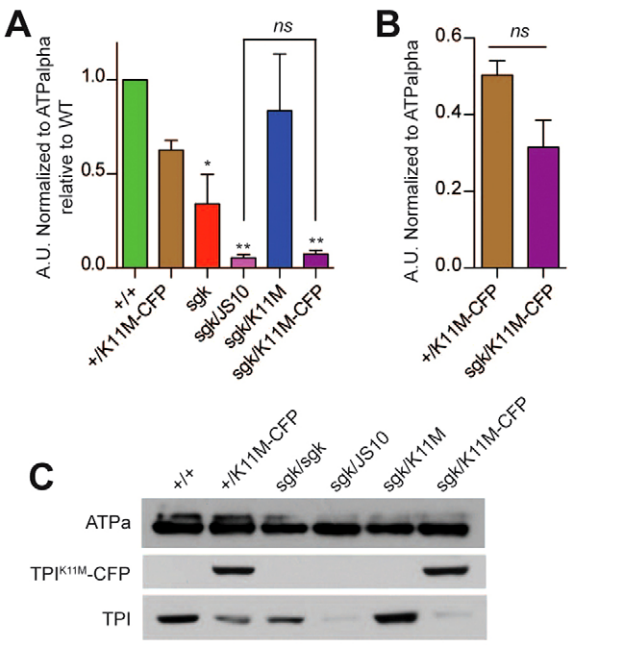

Fig. 4. TPI^{K11M} expression does not prevent the degradation of TPI^{sgk}. (**A**) Quantification of the levels of untagged TPI. TPI^{sgk} complemented with TPI^{K11M} shows elevated levels of total TPI similar to WT. Additionally, *TPI^{sgk}/TPI^{JS10}* has similar levels of TPI to *TPI^{sgk}/TPI$^{K11M\text{-}CFP}$*. $^{**}P<0.01$ and $^{***}P<0.001$ compared to WT; ns indicates no significant change compared with *TPI^{sgk}/TPI^{JS10}*. $n=4$. (**B**) TPI^{sgk} does not induce the degradation of TPI$^{K11M\text{-}CFP}$. Quantification and comparison of the levels of TPI^{K11M}-CFP (shown in C). Student's *t*-test was used to compare the two groups and found no significant difference (ns). $n=4$. Error bars indicate ± s.e.m. (**C**) A representative blot from which the data in A,B were obtained. The loading control used was ATPalpha (Na,K-ATPase).

TPI^{K11M} never exist as a heterodimer. Taken together, these results confirm that *TPI^{K11M}* complements the *TPI^{sgk}* phenotypes independent of isomerase activity demonstrating a non-catalytic function of TPI crucial to the pathogenesis and severity of TPI deficiency.

Discussion

The *sugarkill* model of TPI deficiency used in these experiments is characterized by reduced catalysis and protein stability, characteristics found in several of the more toxic human *TPI* alleles (Hollán et al., 1993; Watanabe et al., 1996; Arya et al., 1997). Similarly, the M80T mutation recapitulates the neurological dysfunction and toxicity exhibited in many of the human patients. Using *Drosophila* we have genomically engineered (GE) the *TPI* locus to make targeted *in vivo* modifications to the endogenous gene. GE allows us to study *TPI* manipulations under endogenous regulatory control, allowing rigorous experiments that would not be feasible with traditional transgenic approaches (Huang et al., 2011; Pollarolo et al., 2011; Venken et al., 2011). The power of GE is born in its capacity to study a gene's function *in vivo* while reducing artifacts due to transgenic overexpression and miss expression. Previous studies analyzing TPI deficiency have primarily utilized human patient erythrocytes, yeast and mammalian cellular expression systems. Although these experimental paradigms are valuable, they do not provide the elegant endogenous genetic control of GE and preclude the examination of *in vivo* phenotypes such as behavior and longevity.

We initiated this study asking whether the presence of the enzyme or its catalytic activity was most important to the pathogenesis of our mutant. Our experiments assessing enzyme activity identified that the M80T substitution in TPI^{sgk} resulted in a ~11-fold reduction in enzyme catalysis with modest changes in substrate affinity (Table 1). This reduction in catalytic activity was more severe than those reported in two human mutations (Orosz et al., 2001; Rodríguez-Almazán et al., 2008), but was not nearly as severe as those modifying crucial catalytic components (Raines et al., 1986; Nickbarg et al., 1988; Casteleijn et al., 2006; Go et al., 2010). An analysis of the TPI enzyme structure taken from *G. gallus* suggested that this mutation might affect isomerase activity through its proximity to several catalytic residues (Fig. 1). These results initially supported a catalytic mechanism of disease pathogenesis, but further experimentation revealed the capacity for an isomerase-inactive isoform of TPI to genetically complement all behavioral and longevity phenotypes of *TPI^{sgk}*. The capacity for a catalytically inactive TPI to rescue a severe variant of TPI deficiency without a change in isomerase activity was striking. Most research on TPI deficiency focuses on two core principles: reduced TPI activity slows glycolysis, and inhibition of TPI leads to a buildup of excess DHAP and henceforth toxic advanced glycation end-products (AGEs) (Orosz et al., 2009). Here we have shown the capacity to rescue animal behavior and longevity without restoring TPI catalysis, making it unlikely that AGEs are playing a significant role in the genesis of our behavioral or longevity phenotypes. Further, the metabolic change detected in our mutant was also not rescued upon attenuation of behavior. These data suggest a new model of TPI function and we propose that this non-catalytic function is crucial to the neurological complications that contribute to TPI deficiency pathogenesis (Fig. 5).

Although glycolytic enzymes are not often thought of as important players in non-metabolic cellular mechanisms, work spanning the past two decades has clearly outlined vital non-metabolic roles for some of these ancient proteins. Glycolytic enzymes have been described in a multitude of different non-catalytic roles, including assistance in assembly and function of the vacuolar-type proton-ATPase by aldolase (Lu et al., 2004; Lu et al., 2007), inhibition of apoptosis through the modulation of Bax, Bak and Bad by hexokinase (Pastorino et al., 2002; Majewski et al., 2004), transcriptional regulation of the histone H2B gene during cell cycle progression by glyceraldehyde 3-phosphate dehydrogenase (Zheng et al., 2003), and the induction of cell motility and invasion through the secretion and binding of glucose 6-phosphate isomerase to the autocrine motility factor receptor gp78 (Niinaka et al., 1998). The potential for glycolytic enzymes to perform crucial functions dramatically independent from their roles in glycolysis is evident (reviewed by Kim and Dang, 2005). Our findings are particularly relevant as TPI is one of the primary targets of nitrotyrosination in Alzheimer's disease and is sequestered in the neurofibrillary tangles in patient brains (Coma et al., 2005; Guix et al., 2009). Sequestration such as this could inhibit a crucial non-catalytic function of TPI, further contributing to the neurological dysfunction known to be associated with tau aggregation and toxic amyloid beta.

Recently TPI has been identified as a target of cyclin dependent kinase 2 (cdk2) (Lee et al., 2010) and arginine methyltransferase 5 (PRMT5) (Kim et al., 2010). Together, these

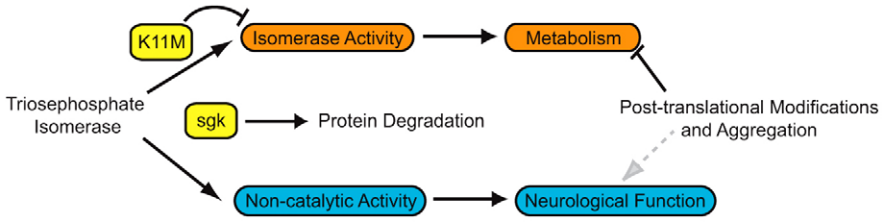

Fig. 5. Model of TPI function and pathogenesis. The results of this study suggest that TPI has catalytic (orange) and non-catalytic (blue) functions. Impairment of TPI function (yellow) was studied *in vivo* using K11M (abolishes catalytic activity) and sgk (leads to protein degradation). The data demonstrate the presence of a non-isomerase TPI function required for normal neural function and suggests that loss of this function underlies neuropathogenesis in TPI deficiency.

studies conclude that TPI is more highly regulated than previously appreciated. Furthermore, it was noted that TPI protein levels could be modulated via methylation (Kim et al., 2010). These results portend the enticing possibility that TPI protein levels are regulated in a cell-cycle-dependent manner, and that its relationship to the cell cycle could be perturbed in TPI-deficient patients experiencing neurological symptoms. Indeed, a relationship has already been well established between cell cycle misregulation and neurodegeneration (reviewed by Khurana and Feany, 2007), and inappropriate regulation of the cell cycle has been described in Alzheimer's disease (Yang et al., 2001). It is clear that further work is needed to define the biological role of post-translational modifications of TPI, and the role of TPI as either a direct or indirect component of the cell cycle.

In conclusion, our data demonstrate the capacity of a catalytically inactive TPI enzyme to genetically complement TPI deficiency behavioral phenotypes independent of changes in bioenergetics or enzyme catalysis. The identification of an isomerase-independent function for this crucial protein opens up new avenues of investigation that will prove crucial to understanding the role of TPI in maintaining normal neural function and TPI deficiency pathogenesis.

Materials and Methods

Animal strains

The *Drosophila w*; P{GawB} 477w-; TM2/TM6B, Tb*^{1} and *y,w/Y, hs-hid; hs-FLP, hs-I-SceI/CyO, hs-hid*; stocks were obtained from Dr Yang Hong. *TPI*^{sgk} is a missense mutation resulting in a Met-to-Thr change at position 80, while *TPI*^{JS10} is a null allele owing to a 1.6 kb deletion of two of the three constitutively expressed exons of the *TPI* locus (Celotto et al., 2006). This numbering uses the established nomenclature for TPI mutations, assuming the start methionine is removed following translation (Orosz et al., 2006); and for consistency all residue numbering in this study uses the same convention. The Cre recombinase stock was used to reduce the locus following homologous recombination and phiC31 integration. The strain used, *y*^{1} *w*^{67c23} *P{y[+mDint2]=Crey}1b; D*/TM3, Sb*^{1}, was obtained from the Bloomington *Drosophila* Stock Center (Bloomington, IN, USA). Care was taken to ensure all animal populations assessed were approximately equivalent mixtures of males and females, with the exception of the *TPI*^{sgk}*/TPI*^{JS10} day 20 behavioral tests – in this genotype males died noticeably faster than females and as a result this small population of survivors consisted mostly of female animals.

Genomic engineering

We performed the *TPI* GE similar to previously published methods (Huang et al., 2008; Huang et al., 2009). Briefly, ~2.6 kb homology arms were generated by PCR amplification to areas 5′ and 3′ of the *TPI* locus. These homology arms were inserted into the pGX-attB vector (Huang et al., 2009) and transferred onto the second chromosome of *w*^{1118} animals using traditional P-element transgenesis. Ends-out homologous recombination was performed and founder lines were molecularly verified. The wild type *TPI* locus was cloned into the *pGE-attB* vector via PCR and verified by sequencing. Founder lines were mated to *vasa-phiC31*$^{ZH-2A}$ animals expressing the integrase on the X chromosome and their progeny injected with pGE-attBTPI^{+}, pGE-attBTPI^{+}-CFP, pGE-attBTPI^{M80T}, pGE-attBTPI^{K11M}, or pGE-attBTPI^{K11M}-CFP constructs. Integration events between *attP* and *attB* elements produce an *attL* and *attR* and reconstitute the target locus. Such events were identified based on the presence of the *w*$^{+}$ phenotype and verified molecularly.

Mutagenesis

Site directed mutagenesis was performed using the QuikChange Lightning Site-Directed Mutagenesis Kit (Agilent Technologies, Santa Clara, CA, USA). Mutagenesis primers were generated (Integrated DNA Technologies, Coralville, IA, USA) to introduce a Lys-to-Met codon change affecting position 11 and a Met-to-Thr codon change affecting position 80 of the protein. Mutagenesis was performed on the *pGE-attBTPI*$^{+}$ plasmid and confirmed by sequencing.

Drosophila TPI purification

The coding sequence for *Drosophila* TPI was cloned into the bacterial expression vector pLC3 using standard techniques. The resulting plasmid directs expression of TPI containing N-terminal His_6- and MBP tags, both of which can be removed with TEV protease. TPI protein was expressed in BL21(DE3) Codon-Plus (RILP) *E. coli* (Agilent Technologies) grown in ZY auto-induction media (Studier, 2005) at room temperature for 24–30 hours. Cells were harvested by centrifugation, lysed via homogenization in 25 mM Tris pH 8.0, 500 mM NaCl, 10% glycerol, 5 mM imidazole, 1 mM β-mercaptoethanol and cleared by centrifugation at 30,000 ***g***. TPI was purified by nickel affinity chromatography followed by overnight TEV protease treatment to cleave the His_6-MBP tag from TPI. A second round of nickel affinity purification was performed to separate the His_6-MBP and TEV protease. TPI protein was further purified using cation-exchange chromatography (HiTrap-QP) followed by gel filtration (Sephacryl S-200, GE Healthcare, Little Chalfont, England, UK). Peak fractions were concentrated to 4–8 mg/ml in 20 mM Tris pH 8.8, 25 mM NaCl, 2.0% glycerol and 1 mM β-mercaptoethanol using a Vivaspin concentrator (GE Healthcare). The purity was >99% as verified by SDS-PAGE. Expression and purification of the *Drosophila* TPI M80T *sgk* mutant was performed as described above.

Enzyme assays

Isomerase activity was determined using an NADH-linked assay as previously detailed (Williams et al., 1999). TPI activity was measured with three different enzyme concentrations of both purified *Drosophila* WT and M80T enzyme. Initial velocity of the enzyme was calculated over a GAP (Sigma-Aldrich, St. Louis, MO, USA) range of 0.94–5.64 mM. All kinetic measurements were performed three times in triplicate by monitoring the absorbance of NADH at 340 nm in a SpectraMax Plus 384 microplate reader (Molecular Devices, Sunnyvale, CA, USA). The assay was performed using 80 µl mixtures containing varied GAP and enzyme concentrations, 0.42 mM NADH (Sigma-Aldrich), and 1 unit glycerol-3-phosphate dehydrogenase (Sigma-Aldrich) in 100 mM triethanolamine (TEA), pH 7.6. Enzyme activity curves were normalized to reactions performed without GAP. Enzyme kinetics were determined by assessing initial velocities taken during the linear phase of each reaction, and the data were fit to the Michaelis–Menten equation using nonlinear regression in Graphpad Prism 5.0b (GraphPad Software, La Jolla, CA, USA).

For lysate assays, animals were collected and aged to day 3 at 25℃ and frozen in liquid nitrogen. Bodies lacking the head and appendages (abdomen and thorax) were isolated after vigorous mechanical shaking of the frozen animals. Tissues lacking eye pigments were used to reduce background absorbance. The bodies were homogenized in 0.75 ml of 1× PBS (2.7 mM KCl, 137 mM NaCl, 2 mM NaH_2PO_4, 10 mM Na_2HPO_4 pH 7.4) with protease inhibitors leupeptin 1:1000 (Acros Organics, Geel, Belgium), pepstatin 1:1000 (Sigma-Aldrich), PMSF 1:100 (Pierce, Rockford, IL, USA). The homogenates were ice bath-sonicated for 10 minutes then centrifuged at 4℃ for 5 minute at 5,000 ***g*** to remove exoskeletal debris. Lysates were diluted to 1 µg/µl in 100 mM TEA, pH 7.6 + inhibitors and TPI enzyme activity was assessed using a linked-enzyme assay, similar to that outlined above. The assay was performed using 80 µl mixtures containing 0.47 mM GAP, 0.42 mM NADH, 1 unit glycerol-3-phosphate dehydrogenase and 30 µg of lysate protein in 100 mM TEA, pH 7.6. Enzyme activity curves were performed three times in triplicate and normalized to reactions performed without GAP. A one-way ANOVA was performed to assess variance and data sets were compared using Tukey's post-hoc analysis.

Behavioral testing and lifespan analysis

Mechanical stress sensitivity was determined by vortexing the animals in a standard media vial for 20 seconds and measuring time to recovery, similar to (Ganetzky and Wu, 1982). Thermal stress sensitivity was assessed by acutely

shifting animals to 38℃ and measuring time to paralysis, as previously described (Palladino et al., 2002; Palladino et al., 2003). All behavioral responses were capped at 600 seconds. Testing days were selected based on previous experience with TPI deficiency progression in *Drosophila* (Celotto et al., 2006). Animal lifespans were performed at 25℃ as previously described (Palladino et al., 2003). Two-way ANOVAs were performed with Bonferroni's post test to compare genotype behavior over time, and lifespans were compared with Log-rank (Mantel–Cox) survival tests.

HPLC phosphoarginine assay

Three sets of 25 animals per genotype were collected and aged to day 3 at 25℃ and frozen in liquid nitrogen. The animals were homogenized in 200 µl 0.6 M perchloric acid and neutralized with 25 µl of 2 M potassium carbonate. The lysates were then centrifuged at 12,000 ***g*** for 10 minutes at 4℃ and the supernatant filtered through a PVDF 0.45 µm spin column (National Scientific, Rockwood, TN, USA) at 12,000 ***g*** for 5 minutes at 4℃ as previously described (Celotto et al., 2011). These extracts were injected onto a Phenomenex Luna 5 µm NH_2 250×4.6 mm column (Torrance, CA, USA) using a Shimadzu high performance liquid chromatography (HPLC) system (Kyoto, Japan) and separated with a 95:5 20 mM KH_2PO_4 pH 2.6: acetonitrile linear mobile phase at a flow rate of 0.6 ml/minute. Arginine (Acros Organics) and phospho-arginine (P-arg) standards were detected at 205 nm, and all samples were measured in triplicate (Celotto et al., 2011). Phospho-arginine standards were generated as previously described (Morrison et al., 1957). Peak analysis was performed using EZStart 7.3 software (Shimadzu), and P-arg levels were normalized to total arginine and compared across genotypes. Retention times for arginine and phospho-arginine were 3.7 minutes and 5.4 minutes, respectively. A one-way ANOVA was performed to assess variance and data sets were compared using Tukey's post-hoc analysis.

Immunoblots

Animals were collected and aged at 29℃. After 24 hours, ten fly heads were collected in triplicate from each genotype and processed as outlined previously (Hrizo and Palladino, 2010). Briefly, the fly heads were ground by pestle in 80 µl 2× SDS–PAGE sample buffer (4% SDS, 4% β-mercaptoethanol, 130 mM Tris–HCl pH 6.8, 20% glycerol) and centrifuged for 5 minutes at 5000 ***g*** to pellet the exoskeleton. Proteins were resolved by SDS–PAGE and transferred onto PVDF membrane. Following treatment in 1% milk PBST, the blots were incubated with anti-TPI (1:5000; rabbit polyclonal FL-249; Santa Cruz Biotechnology, Santa Cruz, CA, USA) or anti-ATPalpha (1:10,000; mouse monoclonal alpha5; Developmental Studies Hybridoma Bank, Iowa City, IA, USA). The blots were washed in PBST, incubated in the appropriate HRP-conjugated secondary antibody, and developed using ECL (Pierce). Densitometric analyses of the scanned films were performed digitally using ImageJ software available from the National Institutes of Health. A one-way ANOVA was performed to assess variance of TPI levels and data sets were compared using Tukey's post-hoc analysis.

Acknowledgements

We thank Dr Yang Hong for fly strains and clones to perform the genomic engineering; the Bloomington Stock center for fly strains; Samula Mula, Henry Liu, Mallory Hensel, Matt Baumgartner, Brian Kosik, Krupa Patel and Alicia Olsen for assistance with the genomic engineering.

Author contributions

B.P.R., K.A.S., A.M.C., and M.J.P. designed the research; B.P.R., K.A.S., S.B.L., and A.M.C. performed the research; C.G.A. and A.P.V. contributed new reagents, B.P.R., C.G.A., A.P.V. and M.J.P. analyzed the data, and B.P.R. and M.J.P. wrote the paper.

Funding

This work was supported by a fellowship from Achievement Rewards for College Scientists: Pittsburgh Chapter [to B.P.R.]; and the National Institutes of Health [grant numbers R01AG027453, R01AG025046, R01GM103369 to M.J.P., R01GM097204 to A.P.V. and T32GM8424-17 to B.P.R.]. Deposited in PMC for release after 12 months.

Supplementary material available online at
http://jcs.biologists.org/lookup/suppl/doi:10.1242/jcs.124586/-/DC1

References

Arya, R., Lalloz, M. R., Bellingham, A. J. and Layton, D. M. (1997). Evidence for founder effect of the Glu104Asp substitution and identification of new mutations in triosephosphate isomerase deficiency. *Hum. Mutat.* **10**, 290-294.

Casteleijn, M. G., Alahuhta, M., Groebel, K., El-Sayed, I., Augustyns, K., Lambeir, A. M., Neubauer, P. and Wierenga, R. K. (2006). Functional role of the conserved active site proline of triosephosphate isomerase. *Biochemistry* **45**, 15483-15494.

Celotto, A. M., Frank, A. C., Seigle, J. L. and Palladino, M. J. (2006). Drosophila model of human inherited triosephosphate isomerase deficiency glycolytic enzymopathy. *Genetics* **174**, 1237-1246.

Celotto, A. M., Chiu, W. K., Van Voorhies, W. and Palladino, M. J. (2011). Modes of metabolic compensation during mitochondrial disease using the Drosophila model of ATP6 dysfunction. *PLoS ONE* **6**, e25823.

Coma, M., Guix, F. X., Uribesalgo, I., Espuña, G., Solé, M., Andreu, D. and Muñoz, F. J. (2005). Lack of oestrogen protection in amyloid-mediated endothelial damage due to protein nitrotyrosination. *Brain* **128**, 1613-1621.

Daar, I. O., Artymiuk, P. J., Phillips, D. C. and Maquat, L. E. (1986). Human triosephosphate isomerase deficiency: a single amino acid substitution results in a thermolabile enzyme. *Proc. Natl. Acad. Sci. USA* **83**, 7903-7907.

Ganetzky, B. and Wu, C. F. (1982). Indirect suppression involving behavioral mutants with altered nerve excitability in Drosophila melanogaster. *Genetics* **100**, 597-614.

Gnerer, J. P., Kreber, R. A. and Ganetzky, B. (2006). wasted away, a Drosophila mutation in triosephosphate isomerase, causes paralysis, neurodegeneration, and early death. *Proc. Natl. Acad. Sci. USA* **103**, 14987-14993.

Go, M. K., Koudelka, A., Amyes, T. L. and Richard, J. P. (2010). Role of Lys-12 in catalysis by triosephosphate isomerase: a two-part substrate approach. *Biochemistry* **49**, 5377-5389.

Gong, W. J. and Golic, K. G. (2003). Ends-out, or replacement, gene targeting in Drosophila. *Proc. Natl. Acad. Sci. USA* **100**, 2556-2561.

Guix, F. X., Ill-Raga, G., Bravo, R., Nakaya, T., de Fabritiis, G., Coma, M., Miscione, G. P., Villà-Freixa, J., Suzuki, T., Fernàndez-Busquets, X. et al. (2009). Amyloid-dependent triosephosphate isomerase nitrotyrosination induces glycation and tau fibrillation. *Brain* **132**, 1335-1345.

Hollán, S., Fujii, H., Hirono, A., Hirono, K., Karro, H., Miwa, S., Harsányi, V., Gyódi, E. and Inselt-Kovács, M. (1993). Hereditary triosephosphate isomerase (TPI) deficiency: two severely affected brothers one with and one without neurological symptoms. *Hum. Genet.* **92**, 486-490.

Hrizo, S. L. and Palladino, M. J. (2010). Hsp70- and Hsp90-mediated proteasomal degradation underlies TPI sugarkill pathogenesis in Drosophila. *Neurobiol. Dis.* **40**, 676-683.

Huang, J., Zhou, W., Watson, A. M., Jan, Y. N. and Hong, Y. (2008). Efficient ends-out gene targeting in Drosophila. *Genetics* **180**, 703-707.

Huang, J., Zhou, W., Dong, W., Watson, A. M. and Hong, Y. (2009). From the Cover: Directed, efficient, and versatile modifications of the Drosophila genome by genomic engineering. *Proc. Natl. Acad. Sci. USA* **106**, 8284-8289.

Huang, J., Huang, L., Chen, Y. J., Austin, E., Devor, C. E., Roegiers, F. and Hong, Y. (2011). Differential regulation of adherens junction dynamics during apical-basal polarization. *J. Cell Sci.* **124**, 4001-4013.

Khurana, V. and Feany, M. B. (2007). Connecting cell-cycle activation to neurodegeneration in Drosophila. *Biochim. Biophys. Acta* **1772**, 446-456.

Kim, J. W. and Dang, C. V. (2005). Multifaceted roles of glycolytic enzymes. *Trends Biochem. Sci.* **30**, 142-150.

Kim, C., Lim, Y., Yoo, B. C., Won, N. H., Kim, S. and Kim, G. (2010). Regulation of post-translational protein arginine methylation during HeLa cell cycle. *Biochim. Biophys. Acta* **1800**, 977-985.

Lambeir, A. M., Opperdoes, F. R. and Wierenga, R. K. (1987). Kinetic properties of triose-phosphate isomerase from Trypanosoma brucei brucei. A comparison with the rabbit muscle and yeast enzymes. *Eur. J. Biochem.* **168**, 69-74.

Lee, W. H., Choi, J. S., Byun, M. R., Koo, K. T., Shin, S., Lee, S. K. and Surh, Y. J. (2010). Functional inactivation of triosephosphate isomerase through phosphorylation during etoposide-induced apoptosis in HeLa cells: potential role of Cdk2. *Toxicology* **278**, 224-228.

Lodi, P. J., Chang, L. C., Knowles, J. R. and Komives, E. A. (1994). Triosephosphate isomerase requires a positively charged active site: the role of lysine-12. *Biochemistry* **33**, 2809-2814.

Lu, M., Sautin, Y. Y., Holliday, L. S. and Gluck, S. L. (2004). The glycolytic enzyme aldolase mediates assembly, expression, and activity of vacuolar H+-ATPase. *J. Biol. Chem.* **279**, 8732-8739.

Lu, M., Ammar, D., Ives, H., Albrecht, F. and Gluck, S. L. (2007). Physical interaction between aldolase and vacuolar H+-ATPase is essential for the assembly and activity of the proton pump. *J. Biol. Chem.* **282**, 24495-24503.

Majewski, N., Nogueira, V., Bhaskar, P., Coy, P. E., Skeen, J. E., Gottlob, K., Chandel, N. S., Thompson, C. B., Robey, R. B. and Hay, N. (2004). Hexokinase-mitochondria interaction mediated by Akt is required to inhibit apoptosis in the presence or absence of Bax and Bak. *Mol. Cell* **16**, 819-830.

Morrison, J. F., Griffiths, D. E. and Ennor, A. H. (1957). The purification and properties of arginine phosphokinase. *Biochem. J.* **65**, 143-153.

Nickbarg, E. B., Davenport, R. C., Petsko, G. A. and Knowles, J. R. (1988). Triosephosphate isomerase: removal of a putatively electrophilic histidine residue results in a subtle change in catalytic mechanism. *Biochemistry* **27**, 5948-5960.

Niinaka, Y., Paku, S., Haga, A., Watanabe, H. and Raz, A. (1998). Expression and secretion of neuroleukin/phosphohexose isomerase/maturation factor as autocrine motility factor by tumor cells. *Cancer Res.* **58**, 2667-2674.

Norledge, B. V., Lambeir, A. M., Abagyan, R. A., Rottmann, A., Fernandez, A. M., Filimonov, V. V., Peter, M. G. and Wierenga, R. K. (2001). Modeling, mutagenesis, and structural studies on the fully conserved phosphate-binding loop

(loop 8) of triosephosphate isomerase: toward a new substrate specificity. *Proteins* **42**, 383-389.

Orosz, F., Oláh, J., Alvarez, M., Keseru, G. M., Szabó, B., Wágner, G., Kovári, Z., Horányi, M., Baróti, K., Martial, J. A. et al. (2001). Distinct behavior of mutant triosephosphate isomerase in hemolysate and in isolated form: molecular basis of enzyme deficiency. *Blood* **98**, 3106-3112.

Orosz, F., Oláh, J. and Ovádi, J. (2006). Triosephosphate isomerase deficiency: facts and doubts. *IUBMB Life* **58**, 703-715.

Orosz, F., Oláh, J. and Ovádi, J. (2009). Triosephosphate isomerase deficiency: new insights into an enigmatic disease. *Biochim. Biophys. Acta* **1792**, 1168-1174.

Palladino, M. J., Hadley, T. J. and Ganetzky, B. (2002). Temperature-sensitive paralytic mutants are enriched for those causing neurodegeneration in Drosophila. *Genetics* **161**, 1197-1208.

Palladino, M. J., Bower, J. E., Kreber, R. and Ganetzky, B. (2003). Neural dysfunction and neurodegeneration in Drosophila Na+/K+ ATPase alpha subunit mutants. *J. Neurosci.* **23**, 1276-1286.

Pastorino, J. G., Shulga, N. and Hoek, J. B. (2002). Mitochondrial binding of hexokinase II inhibits Bax-induced cytochrome c release and apoptosis. *J. Biol. Chem.* **277**, 7610-7618.

Pollarolo, G., Schulz, J. G., Munck, S. and Dotti, C. G. (2011). Cytokinesis remnants define first neuronal asymmetry in vivo. *Nat. Neurosci.* **14**, 1525-1533.

Raines, R. T., Sutton, E. L., Straus, D. R., Gilbert, W. and Knowles, J. R. (1986). Reaction energetics of a mutant triosephosphate isomerase in which the active-site glutamate has been changed to aspartate. *Biochemistry* **25**, 7142-7154.

Rodríguez-Almazán, C., Arreola, R., Rodríguez-Larrea, D., Aguirre-López, B., de Gómez-Puyou, M. T., Pérez-Montfort, R., Costas, M., Gómez-Puyou, A. and Torres-Larios, A. (2008). Structural basis of human triosephosphate isomerase deficiency: mutation E104D is related to alterations of a conserved water network at the dimer interface. *J. Biol. Chem.* **283**, 23254-23263.

Rong, Y. S. and Golic, K. G. (2000). Gene targeting by homologous recombination in Drosophila. *Science* **288**, 2013-2018.

Schneider, A. S. (2000). Triosephosphate isomerase deficiency: historical perspectives and molecular aspects. *Baillieres Best Pract. Res. Clin. Haematol.* **13**, 119-140.

Seigle, J. L., Celotto, A. M. and Palladino, M. J. (2008). Degradation of functional triose phosphate isomerase protein underlies sugarkill pathology. *Genetics* **179**, 855-862.

Studier, F. W. (2005). Protein production by auto-induction in high density shaking cultures. *Protein Expr. Purif.* **41**, 207-234.

Venken, K. J., Simpson, J. H. and Bellen, H. J. (2011). Genetic manipulation of genes and cells in the nervous system of the fruit fly. *Neuron* **72**, 202-230.

Viant, M. R., Rosenblum, E. S. and Tjeerdema, R. S. (2001). Optimized method for the determination of phosphoarginine in abalone tissue by high-performance liquid chromatography. *J. Chromatogr. B Biomed. Sci. Appl.* **765**, 107-111.

Watanabe, M., Zingg, B. C. and Mohrenweiser, H. W. (1996). Molecular analysis of a series of alleles in humans with reduced activity at the triosephosphate isomerase locus. *Am. J. Hum. Genet.* **58**, 308-316.

Wierenga, R. K., Kapetaniou, E. G. and Venkatesan, R. (2010). Triosephosphate isomerase: a highly evolved biocatalyst. *Cell. Mol. Life Sci.* **67**, 3961-3982.

Williams, J. C., Zeelen, J. P., Neubauer, G., Vriend, G., Backmann, J., Michels, P. A., Lambeir, A. M. and Wierenga, R. K. (1999). Structural and mutagenesis studies of leishmania triosephosphate isomerase: a point mutation can convert a mesophilic enzyme into a superstable enzyme without losing catalytic power. *Protein Eng.* **12**, 243-250.

Yang, Y., Geldmacher, D. S. and Herrup, K. (2001). DNA replication precedes neuronal cell death in Alzheimer's disease. *J. Neurosci.* **21**, 2661-2668.

Zhang, Z., Sugio, S., Komives, E. A., Liu, K. D., Knowles, J. R., Petsko, G. A. and Ringe, D. (1994). Crystal structure of recombinant chicken triosephosphate isomerase-phosphoglycolohydroxamate complex at 1.8-A resolution. *Biochemistry* **33**, 2830-2837.

Zheng, L., Roeder, R. G. and Luo, Y. (2003). S phase activation of the histone H2B promoter by OCA-S, a coactivator complex that contains GAPDH as a key component. *Cell* **114**, 255-266.